WALL FLAMES AND IMPLICATIONS FOR UPWARD FLAME SPREAD

by

James Quintiere and Margaret Harkleroad
Center for Fire Research
National Bureau of Standards
Gaithersburg, MD 20899, USA
and
Yuji Hasemi
Building Research Institute
Tsukuba-gun, Ibaraki
Japan

Reprinted from the Combustion Science and Technology,Vol. 48, No. 3/4, 191-222, 1986.

Combust. Sci. and Tech., 1986, Vol. 48, pp. 191–222
0010-2202/86/4804-0191$25.00/0

Wall Flames and Implications for Upward Flame Spread

JAMES QUINTIERE and MARGARET HARKLEROAD *Center for Fire Research, National Bureau of Standards, Gaithersburg, MD 20899*
YUJI HASEMI *Building Research Institute, Tsukuba-gun, Ibaraki Pref., Japan*

(Received May 5, 1985; in final form September 19, 1985)

Abstract—New concepts are addressed for predicting the flame spread on materials from laboratory measurements. It focuses on heat transfer which precipitates and precedes upward flame spread on a vertical surface. Six materials have been featured in this study as well as in past related studies. Their flame spread properties are presented. In this particular study heat transfer and flame height results are presented for wall samples burned at varying levels of external irradiance. Also complementary results are presented for methane line burner wall fires. An approximate theoretical analysis is included to serve as a guide to identifying the important variables and their relationship for correlation purposes. Experimental results yield flame height proportional to energy release rate to the 2/3 power, and wall heat flux distributions are roughly correlated in terms of distance divided by flame height. These correlations appear to at least hold for the scale of these experiments: flame heights of 0.3 to 1.4 m.

INTRODUCTION

The flammability of materials is usually assessed by means of its relative performance in a standard test. Various test methods dominate practice in different countries, but no common denominator or conversion factor exists to relate their results. Indeed, the rationales for their conception, or their intended application, probably differ from test to test. Consequently success at correlating their results with actual fire behavior must be viewed with scrutiny. Some examples of the results of such exercises have been reported (Quintiere, 1982; Parker, 1982; Quintiere, 1985). In those analyses some factors, such as energy release, material thermal properties, and ignition temperature, have been discussed in terms of their relationship to fire growth and possible correlation relationships. It should be apparent, however, that different fire scenarios will warrant different factors. Hence only through analysis and the means of acquiring appropriate data will successful correlations be likely.

One approach, which circumvents analysis, is physical scale modeling. For fire problems similitude modeling is incomplete. Nevertheless, "pressure" modeling does offer a viable alternative, and Alpert (1983) has recently demonstrated its characteristics for wall fires. In that study materials were burned in various small-scale configurations at environmental pressure levels above a normal atmosphere.

Of course, both scaling and analytic approaches to wall fires must match full-scale performance in various settings. Full-scale "data-bases" include post-crash fire growth within aircraft cabins by Sarkos *et al.* (1982), studies in support of a standard room fire test in the United States by Lee (1984), and similar work on a French corner test for wall-linings by Hognon (1983). Although some attempts at predicting fire growth on room surface linings have been put forth by Smith (1981) and Steckler (1983), these are either incomplete or contain empirical aspects. In order to develop the basis for such room fire growth models further, a more systematic approach is being pursued.

One aspect of fire growth on a wall surface is the flame spread component itself. Needless to say that the burning rate, its behavior over time and its response to the room environment, is not unimportant. For the flame spread component, the simplest analytical description is adopted to, at least, organize the attack on this problem. In that sense, spread is subdivided into concurrent flow spread (in the direction of the local gas flow) and opposed flow spread (opposite to the local gas flow). Also, both cases are treated as applicable to a thermally thick solid, which can be shown justifiable for most common materials of thicknesses greater than 1 mm. For opposed flow spread deRis (1969) obtains

$$V = \frac{(k\rho c)_g V_g (T_f - T_{ig})^2}{(k\rho c)(T_{ig} - T_s)^2}, \tag{1}$$

in which $k\rho c$ are the solid's thermal properties, $(k\rho c)_g$ are the corresponding gas properties, V_g is the opposed flow speed, T_f the adiabatic flame temperature, T_{ig} the ignition or pyrolysis temperature, and T_s the upstream solid surface temperature. The corresponding concurrent flow case, given by Sibulkin and Kim (1977), is

$$V = \frac{(\dot{q}_f'')^2 \delta_f}{k\rho c (T_{ig} - T_s)^2}, \tag{2}$$

where $\dot{q}_f''$ is the maximum heat flux at the pyrolysis front, and δ_f is an effective flame heat transfer distance measured from the end of the pyrolysis region. If we consider $\dot{q}_f''$ to be uniform over a flame extension region δ_f and zero beyond, then we should modify Eq. (2) by multiplying $k\rho c$ by $\pi/4$. In previous studies by Harkleroad *et al.* (1983) and Quintiere *et al.* (1983) it was shown how $k\rho c$, T_{ig} and the numerator of Eq. (1) could be estimated from an experimental technique. Recently, such values have been tabulated for a wide range of materials (Quintiere and Harkleroad, 1984). Consequently, knowledge of $\dot{q}_f''$ and δ_f in Eq. (2) would then complete the required information for wall flame spread.

Thus, an experimental apparatus was designed and constructed to measure the heat flux and flame height above a burning wall section. Provision was made to include external irradiation since most materials do not support sustained combustion on their own. Also provisions were made to substitute a horizontal porous gas burner for the burning vertical slab. This substitution would provide steady-state data in contrast to the unsteady burning of the materials. Hence the gas burner data will complement the material data. Indeed, it helped to guide the analysis and those gas burner results are more extensively discussed by Hasemi (1984). The only other available data on heat transfer to the wall region above the pyrolysis zone were taken by Ahmad and Faeth (1979) for steady liquid-saturated wick fires.

DISCUSSION

Experiments

The experimental set-up of Ahmad and Faeth (1979) was used as a guide in this work, but a radiant source was added. A schematic of the apparatus developed is shown in Figure 1, and a photograph of it is shown in Figure 2. The sample section was nominally 28×28 cm and exposed to radiation from two larger gas-fired porous ceramic heaters. The heaters operated at glowing temperatures which could be

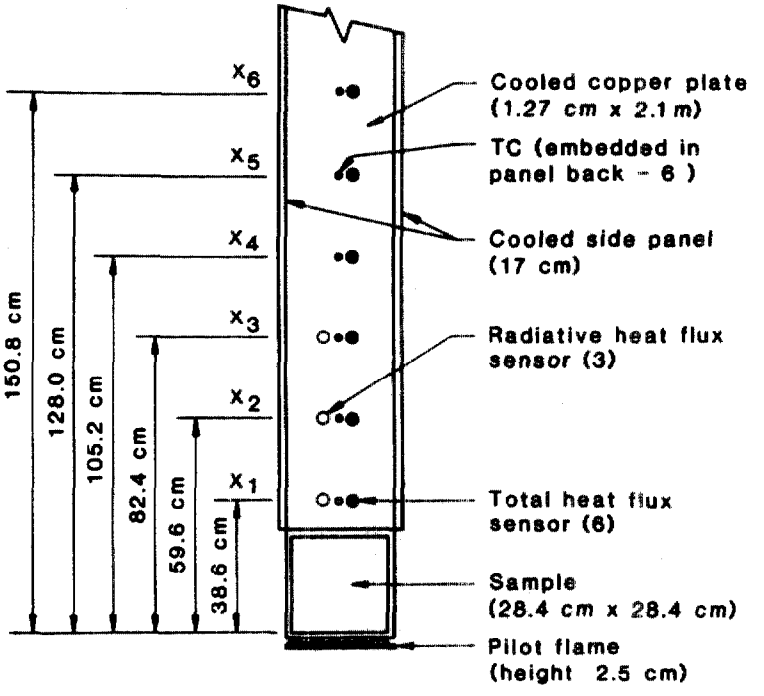

FIGURE 1 Schematic of apparatus.

varied by changing the air and natural gas supply rates. They were located at each side so that the sample could be viewed normal to its surface. This location and their operating characteristics permitted an irradiance level at the sample surface of nominally 1 to 4 W/cm^2. A "Gardon" foil-type heat flux transducer was used to measure the incident flux at the center of an inert sample board. Uniformity over the sample area was within ten percent and the weighted-average irradiance was 0.94 of the center value.

Above the sample was a flush-mounted contiguous copper water-cooled plate with provision for monitoring incident heat flux at the locations shown in Figure 1. Two types of sensors were used—a total heat flux Gardon-type sensor, and an ellipsoidal-type radiometer similar to that described by Chedraille and Brand (1972). Because of calibration uncertainties in this application, the radiometer data will not be presented here. Also an analysis (Appendix A) of the Gardon gage response to convective heat transfer, for a uniform convective heat transfer coefficient (h) over the foil disc, yielded a slight effect of h on the calibration for the sensor used. Moreover, the copper plate was maintained at a nominal temperature of 60°C along with the sensors to prevent condensates from depositing. Cooled side-plates were also included to form a channel and restrict side flow into the flames and preserve two-dimensionality of the boundary layer flow over the plate.

The material to be measured was mounted in an iron-frame holder which could very quickly be inserted in position after the inert sample board was removed. A horizontal copper tube with a line of holes formed a diffusion burner at the base of the sample. This exposed the sample to an ignition pilot flame of approximately 1 cm

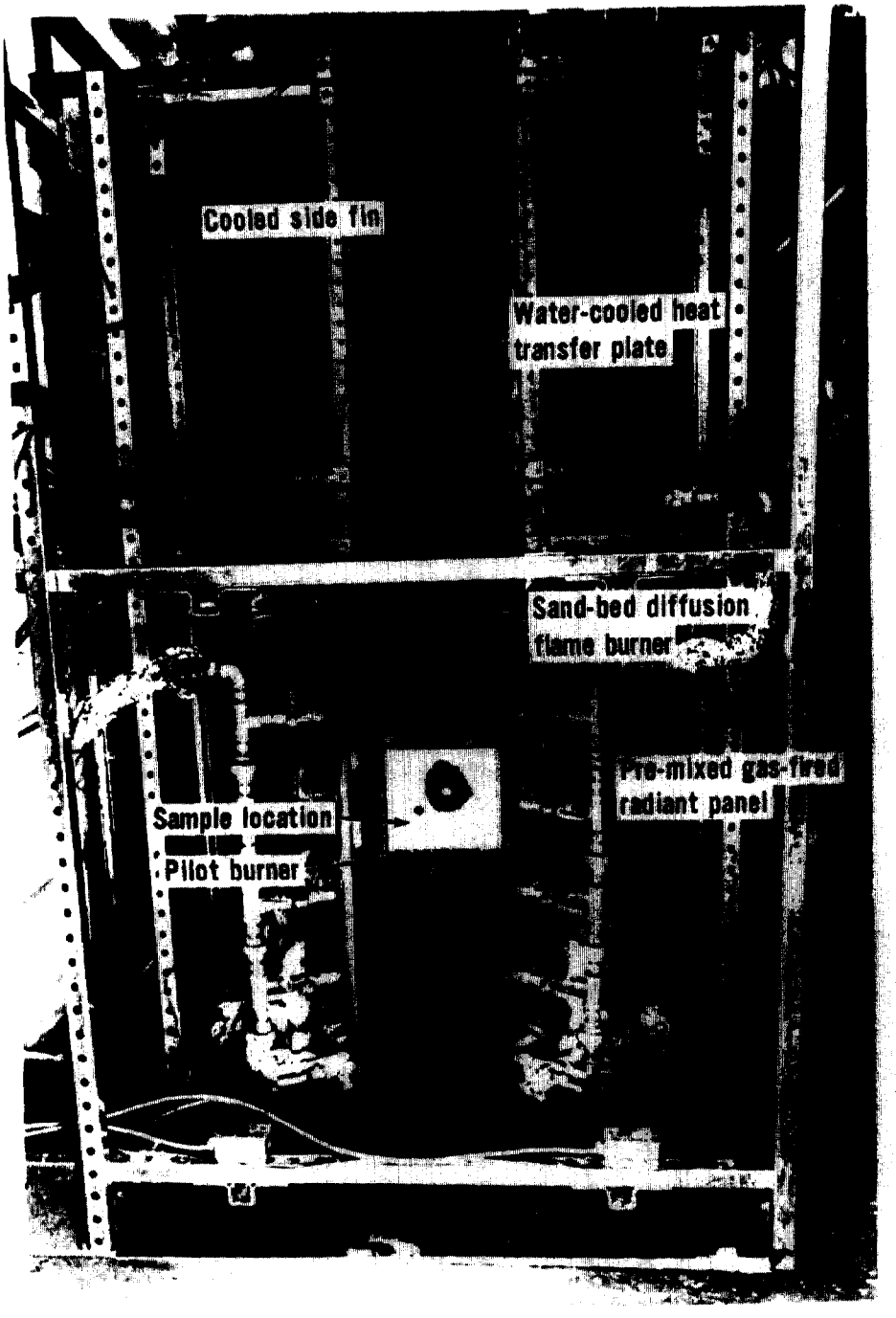

FIGURE 2 Photograph of apparatus.

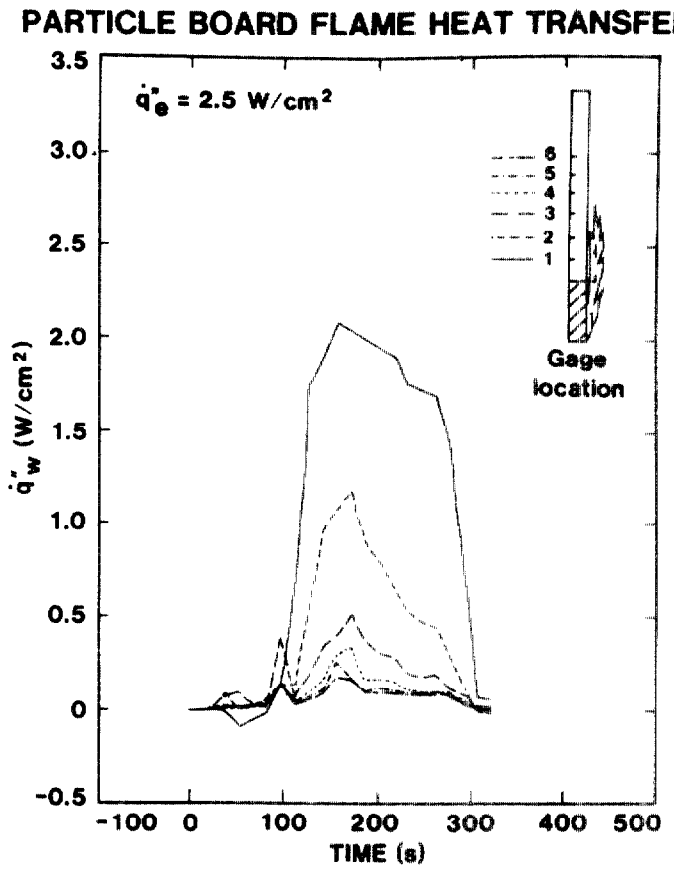

FIGURE 3 Wall heat flux for particleboard irradiated at 2.5 W/cm².

height with a rapidly decreasing heat flux with distance from a maximum of roughly 2 W/cm² at the lower edge of the sample. Thus this pilot flame heated the lower edge of the sample in addition to the applied external radiant heat flux. Nevertheless, the radiant flux was prevalent over most of the sample surface and was the dominant factor in controlling the burning rate. The ignition behavior was controlled by both the applied radiative heat flux and the pilot flame heat flux.

The procedure for conducting the experiment was to set the irradiance level, wait until it stabilized, then insert the sample. A video record was made along with automatic data recording and storage on a computer disc. Signals from the heat flux sensors and thermocouples were scanned and averaged over 10 to 15 s intervals, and their averages stored at these time intervals. The experiment was continued until flaming combustion ceased. The flame height records were deduced by observation of the video recordings and a "flame tip" height was based on the distance to the uppermost position of the luminous flames. A height over which continuous flaming occurred was also recorded, but this was more difficult to observe with consistency and did not always occur above the sample's pyrolysis region. A typical result showing the measured incident total heat flux at the six positions and the corresponding

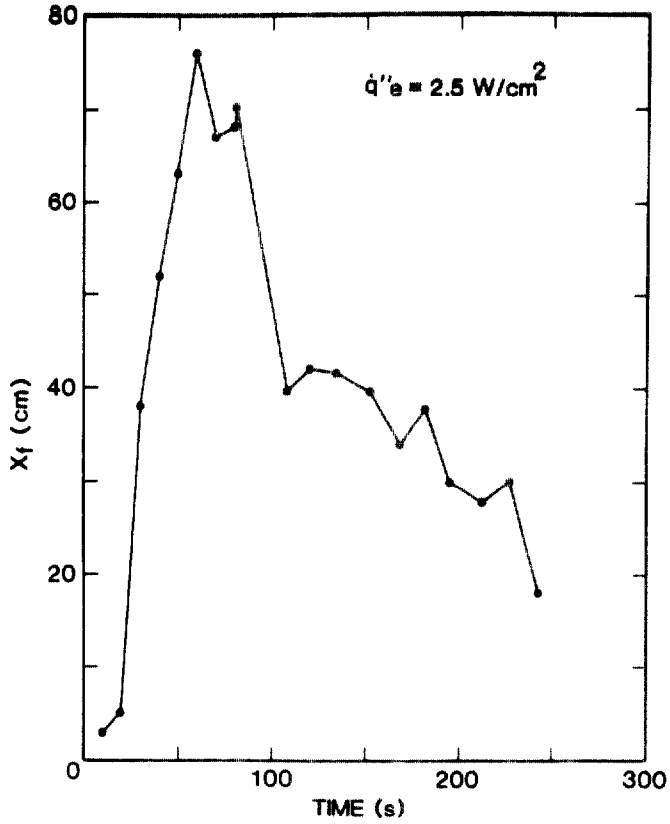

FIGURE 4 Flame height (to tips) for particleboard irradiated at 2.5 W/cm^2.

flame tip height as a function of time is shown in Figures 3 ($t=0$ corresponds to start) and 4 ($t=0$ corresponds to ignition), respectively. It should be noted that the unshielded radiant flux from the heaters was subtracted from the flux measurements so as to yield just the flame heat flux. This superposition view point was justified by the expectation that the flame is likely to be optically thin, and by measurements with a natural gas flame simulating the sample flame. The natural gas diffusion flame was initiated by a horizontal porous burner at the base of the heat transfer plate.

Theoretical Aspects

Before proceeding to analyze and report the results, it was felt necessary to establish a theoretical basis for analysis. The most relevant previous study was by Ahmad and Faeth (1979) who correlated their heat flux data using a turbulent flame-sheet model based on convective heating alone. Moreover, their measured heat flux values above the pyrolysis zone for alcohol-saturated wall fires show a convective component of nearly 80 to 90 percent. Also the heat flux in the flame region was nearly constant, then sharply dropped off as $x^{-7/3}$ approximately. In contrast, the work by Orloff *et al.* (1975) for flame spread on polymethyl-methacrylate shows a radiative

component of 50 to 75 percent. Thus, the composition of this heat flux is expected to be at least material and scale dependent.

Another useful background result is that the flame height appears to be solely dependent on energy release rate for wall fires. This was proposed by Delichatsios (1984) and indeed was demonstrated recently by Hasemi (1984). More recently Delichatsios (1984a) developed a more detailed solution to the wall fire problem. His integral solution addresses both the pyrolyzing region and the wall region above. It contains an improved turbulence model which yields the proper convective heat flux response, and treats the radiative component by an optically thin flame model with specified flame temperature and absorption coefficient. (A description of the optically thin homogeneous flame model is given in Appendix B.) His formulation required a numerical solution whose result he fitted to functional correlations for mass pyrolysis rate and flame height.

As an alternative to reliance on numerical solutions to this problem, an analytical solution was obtained for a simplified, but representative, version of a wall fire. This approach sacrifices some exact features of radiation and turbulence, but is comprehensive in addressing the essential phenomena. Moreover, it at least would provide qualitative and consistent relationships for the significant variables. The primary

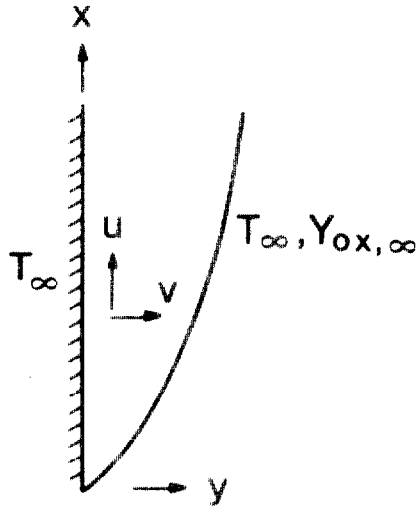

FIGURE 5 Combusting boundary layer problem.

features of this model for a line fuel-source at the wall (Figure 5) are summarized below:

1) The medium is considered a single fluid with combustion energy release set proportional to air entrained into the boundary layer.

2) An optically thin flame is considered with the radiated heat transfer set proportional to the local energy release rate.

3) Simple wall turbulence relationships are utilized (Liburdy and Faeth, 1978) which only apply for high Reynolds numbers.

4) An integral solution is obtained for the 2-D compressible boundary layer equations based on simple polynomial functions.

The full details of this analysis are given in Appendix C. Based on its solution, results for flame height and wall heat flux will be derived.

Flame length An expression for flame length can be derived by assuming that the reaction zone ends when the fuel is completely consumed. That is, the entrainment rate of oxygen primarily controls the flame length. This can be expressed as

$$\int_0^x Y_{ox,\infty}(-\rho v)_{y\to\infty}\,dx = \varepsilon r\dot{m}', \tag{3}$$

where x_f is the flame length, r is the stoichiometric oxygen to fuel mass ratio, $\dot{m}$ is the fuel supply rate and ε is a mixing factor which depends on the fluid dynamics of the flame. From Eq. (3) together with Eqs. (C-15), (C-19) and (C-25) and also by realizing that

$$r\dot{m}' = \dot{E}'/\Delta H_{ox}, \tag{4}$$

where $\dot{E}'$ is the energy release rate per unit width, it follows that

$$x_f = \left(\frac{1.5\varepsilon\dot{E}'}{\rho_\infty Y_{ox,\infty}\Delta H_{ox} a C_e u_0}\right)^{2/3}. \tag{5}$$

Delichatsios (1984) finds, for turbulent wall flames,

$$x_f = 4.65\left(\frac{\dot{E}'}{c_p T_\infty \rho_\infty \sqrt{g}}\right)^{2/3}, \tag{6}$$

which is functionally similar to Eq. (5) by substitution of Eq. (C-27) for u_0. Hasemi (1984) finds the coefficient for Eq. (6) is 6.1 for methane line-burner flames against a wall when x_f pertains to the height of the uppermost flame tips. Hasemi (1984) obtains 2.9 as the coefficient for the height of the continuous flame region. In all cases, these coefficients have been empirically selected.

Wall heat flux An expression for wall heat transfer over the flaming zone can also be derived. From Eqs. (C-7), (C-8), (C-9), (C-19) and (C-23)

$$\dot{q}_{w,r}'' = \frac{0.306\rho_\infty Y_{ox,\infty}\Delta H_{ox}\chi_r u_0 \delta_0 x^{1/2}}{\varepsilon}, \tag{7a}$$

and from Eqs. (C-17), (C-18), (C-19)

$$\dot{q}_{w,c}'' = \frac{C_f}{2Pr^{2/3}}\rho_\infty c_p u_m \theta_m = \frac{C_f}{2Pr^{2/3}}\rho_\infty c_p ab\theta_0 u_0 x^{1/2}. \tag{7b}$$

The total wall flux is

$$\dot{q}_w'' = \rho_\infty u_0\left[\frac{abC_f c_p\theta_0}{2Pr^{2/3}} + \frac{0.306\chi_r Y_{ox,\infty}\Delta H_{ox}\delta_0}{\varepsilon}\right]x^{1/2}. \tag{8}$$

It will be of interest to introduce dimensionless terms and x_f seems to be an appropriate normalizing factor for x. Therefore,

$$\dot{q}_w'' = \beta(x/x_f)^{1/2}, \tag{9a}$$

where

$$\beta = \rho_\infty u_0 \left[\frac{abC_f c_p \theta_0}{2Pr^{2/3}} + \frac{0.306\chi_r Y_{ox,\infty} \Delta H_{ox} \delta_0}{\varepsilon}\right]\left[\frac{1.5\varepsilon \dot{E}'}{\rho_\infty Y_{ox,\infty} \Delta H_{ox} aC_e u_0}\right]^{1/3}. \tag{9b}$$

Equation (9) suggests that β depends weakly on $\dot{E}'$ and $\dot{q}_w''$ increases with x/x_f to the 1/2 power in the reacting zone. The motivation for expressing the heat flux in this form is to examine the extent of similarity in the flame zone. Indeed, this strategy of plotting $\dot{q}_w''$ as a function of x/x_f was used in examining the data and showed remarkable universality. Although it will be shown that Eq. (9) does not follow the data well, its value is in representing the wall heat flux in terms of measurable quantities; namely, $\dot{E}'$ and χ_r. These dependencies need to be further resolved through experimental correlations and more complete theoretical analyses incorporating better models for radiation and wall turbulence. It should be noted that the theoretical results for $\dot{q}_w''$ by Ahmad and Faeth (1979) give a dependence of $x^{0.2}$ in the wall pyrolysis region and give a slightly concave downward dependence in the combusting region downstream. Moreover, analogous turbulent natural convection results might suggest that the heat flux be constant and independent of x.

The numerical solution by Delichatsios (1984a) does yield a constant convective wall heat flux and his full solution with flame radiation bears closer attention with our data. Hence the heat flux result derived here is lacking in the correct x dependence.

Flame spread Although flame spread rate was not explicitly addressed in the experiments, some estimates of flame spread rates could be made with the data. A starting point for this analysis would be Eq. (2); however, the burn-out of the material must also be addressed. Coordinates are shown in Figure 6 which depict the location

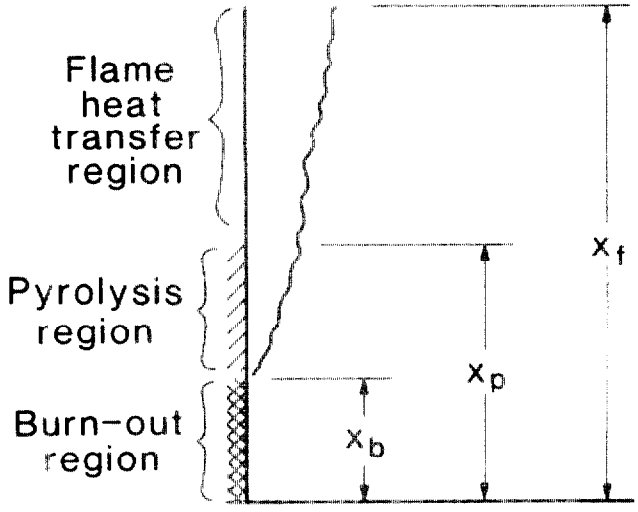

FIGURE 6 Flame spread problem.

of the burn-out front x_b, the pyrolysis front x_p, and the flame tip position x_f—all measured from the leading edge of the solid. Expressions for x_p and x_b can be derived from kinematic arguments by assuming that the front velocity is slowly varying in time. For example, the pyrolysis front velocity can be approximated as

$$V_p = \frac{dx_p}{dt} \cong \frac{x_p(t+t_f)-x_p(t)}{t_f} = \frac{x_f(t)-x_p(t)}{t_f}, \tag{10a}$$

where t_f is the time for the pyrolysis front to move across the flame heat transfer region, $x_f(t)-x_p(t)$. Thus, $x_p(t+t_f)$ will coincide with $x_f(t)$ when the initial surface temperature T_s has been raised to T_{ig} by a constant flame heat flux to the wall $\dot{q}_w''$. From one-dimensional heat conduction theory, it follows that under these conditions for a semi-infinite solid

$$t_f \cong k\rho c[(T_{ig}-T_s)/\dot{q}_w'']^2. \tag{10b}$$

Hence Eq. (10) is identical to the more rigorously derived expression given by Eq. (2).

In a parallel manner, an expression for the burn-out front velocity can be derived. By a difference approximation

$$V_b = \frac{dx_b}{dt} \cong \frac{x_b(t+t_b)-x_b(t)}{t_b} = \frac{x_p(t)-x_b(t)}{t_b}, \tag{11a}$$

where t_b is the duration of burning at a given position x. Thus, by the definition of t_b the burn-out front x_b coincides with $x_p(t)$ when $t=t+t_b$. If t_b is independent of x or slowly varying with x, then by definition, since burning commences at $x_p(t)$ at time t, it follows that $x_b(t+t_b)$ coincides with $x=x_p(t)$ at time $t+t_b$. Also if m represents the volatizable mass, then the burn-out time is defined by

$$\int_0^{t_b} \dot{m}''(x)\,dt = m''. \tag{11b}$$

In general, both t_f and t_b can depend on x, but will be considered as constants in the subsequent illustrative analysis. Appropriate initial conditions are also necessary and can be considered as follows. In any real problem of upward spread, an ignition process will precede flame spread. The ignition source may be a radiative source, a flame source, and transient or constant in application. In any case, at time $t=0$ (ignition), some finite region x_{p_0} of material will be undergoing pyrolysis. Let us assume that the ignition source is removed at $t=0$ also. Furthermore, let us consider a linearized version of Eq. (5) to permit ease in illustrating some solution characteristics, *i.e.*,

$$x_f = k_f\,\dot{E};\ x_p \quad \text{for} \quad t < t_b \quad \text{and} \quad x_f - x_b = k_f\,\dot{E}''(x_p - x_b) \quad \text{for} \quad t > t_b.$$

It can be shown from Eq. (10a) that for $o < t < t_b$,

$$x_p = x_{p_0} \exp[(k_f \dot{E}'' - 1)t/t_f] \tag{12a}$$

and for $t > t_b$ using Eqs. (10a) and (10b) with

$$x_p = x_{p_1} \quad \text{and} \quad x_b = x_{p_0} \quad \text{at} \quad t = t_b,$$
$$x_p - x_b = (x_{p_1} - x_{p_0}) \exp\{[k_f \dot{E}'' - (t_f/t_b) - 1](t-t_b)/t_f\}, \tag{12b}$$

TABLE I

Flame heat transfer characteristics (80 percent average peak)

Material	$\dot{q}_e''$ (W/cm²)	$\dot{q}_1''$ (W/cm²)	$\dot{q}_2''$ (W/cm²)	$\dot{q}_3''$ (W/cm²)	$\dot{q}_4''$ (W/cm²)	$\dot{q}_5''$ (W/cm²)	$\dot{q}_6''$ (W/cm²)	t_b (s)	E'' (kW/m²)	x_f (cm)
Douglas Fir particleboard	1.7[a]	1.71	0.72	0.29	0.15	0.08	0.06	432	140	66
	1.7	1.72	0.73	0.30	0.15	0.09	0.07	209	140	73
	2.5	1.88	0.76	0.30	0.17	0.12	0.11	209	165	61
	3.5	1.79	0.94	0.35	0.16	0.10	0.08	404	195	90
Flexible foam	1.8	2.62	1.84	1.01	0.51	0.31	0.22	72	525	116
	2.5	2.35	1.46	0.70	0.30	0.19	0.13	57	570	96
	3.5[b]	1.99	0.98	0.43	0.22	0.14	0.11	45	645	110
	3.5[b]	2.3	1.18	0.50	0.28	0.18	0.14	47	645	112
Carpet (nylon/wool blend)	2.5	1.98	1.20	0.70	0.34	0.20	0.13	130	75	88
	3.0	2.63	1.69	0.75	0.36	0.20	0.14	101	160	105
	3.0[c]	1.89	0.84	0.27	0.14	0.08	0.08	- -	180	67
	3.6	2.65	1.46	0.65	0.33	0.19	0.15	104	220	39
Foam, rigid	1.9	0.51	0.08	0.04	0.02	0.01	0.01	28	110	39
	2.4	1.05	0.20	0.08	0.05	0.03	0.02	110	130	39
	3.0	1.12	0.20	0.08	0.05	0.04	0.03	137	150	43
	3.0[b]	1.15	0.22	0.10	0.05	0.04	0.03	143	150	42
PMMA	1.5	2.16	2.13	1.59	0.93	0.46	0.30	1664	400	125
	1.7	2.40	2.27	1.71	0.99	0.51	0.32	1558	505	138
	2.4	1.96	2.51	2.14	1.42	0.82	0.51	1331	590	156
	3.0	2.14	2.64	1.96	1.47	0.91	0.63	1112	705	167
Aircraft panel, epoxy fiberite	2.5	0.80	0.30	0.12	0.07	0.04	0.03	43	40	68
	3.0	1.12	0.29	0.10	0.05	0.04	0.03	29	55	48
	3.7	1.06	0.33	0.13	0.07	0.05	0.04	28	80	61

[a]Specimen burns, extinguishes, re-ignites—results from first burn period.
[b]Energy release rate from horizontal burn configuration.
[c]Sample fell from holder after peak burn.

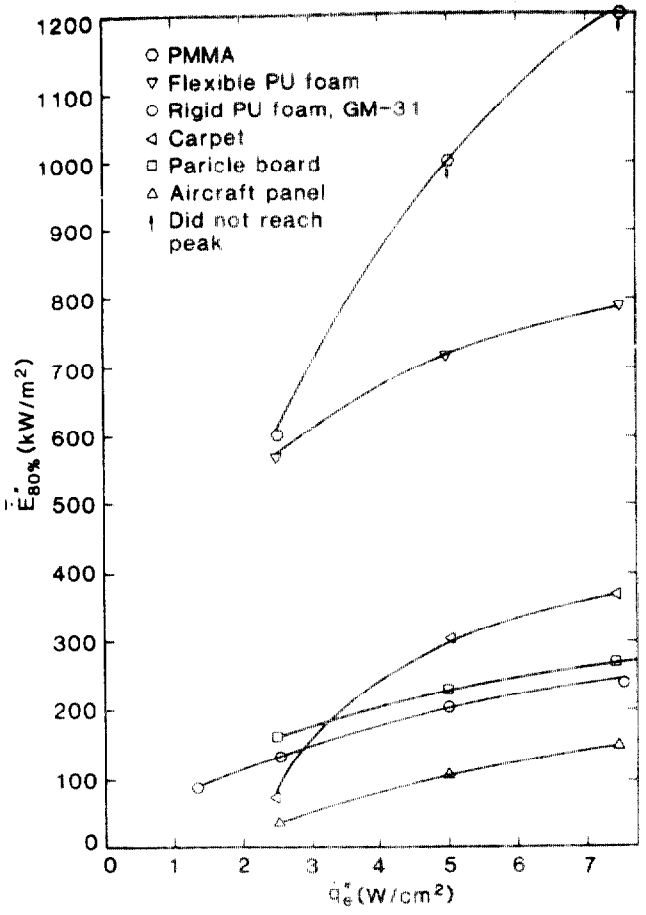

FIGURE 7 Peak energy release rates (Walton and Twilley, 1984).

where $\dot{E}''$ has been assumed constant over the burn time t_b. These results should be viewed as qualitative, but they show the importance of $\dot{E}''$ and t_f/t_b in spread. Indeed, a recent more rigorous analysis by Saito *et al.* (1985) also shows the prominence of these terms. Moreover, Eq. (12b) shows that the spread rate will only be acceleratory provided $k_f\dot{E}''-t_f/t_b>1$. Thus a criterion for self-propagation or the conditions necessary for such is revealed.

RESULTS AND ANALYSIS

The transient aspect of burning materials is difficult to analyze because their degradation behavior is not generally understood. For example, charring, melting, shrinking and significant regressing were all observed among the samples tested. Transient effects in the gas-phase are very fast, so that a quasi-steady analysis is justifiable for

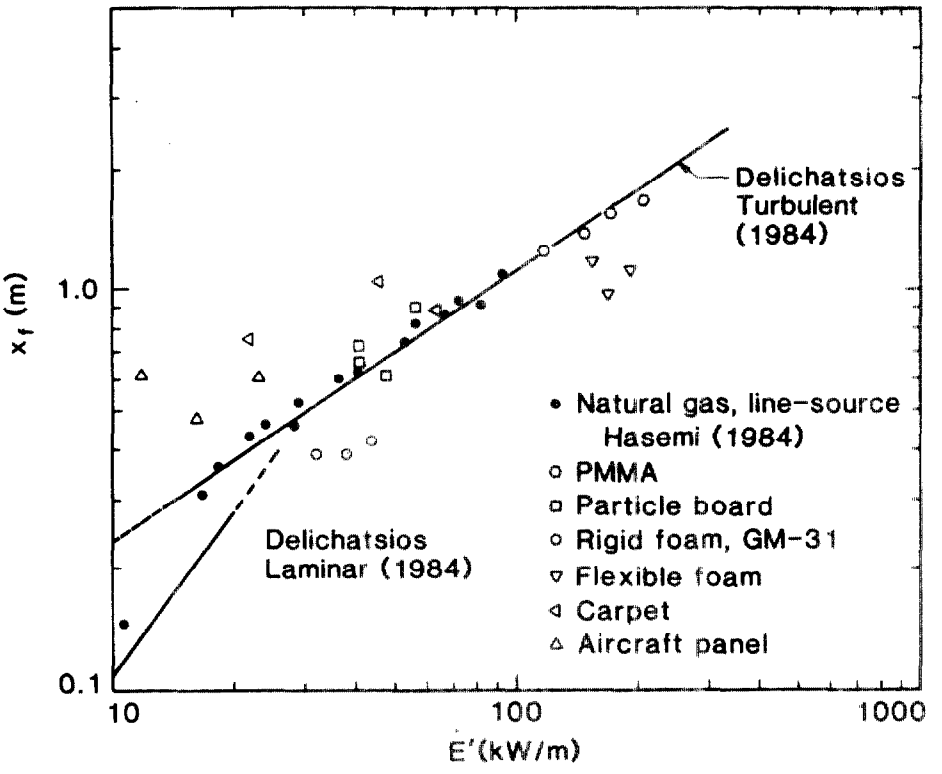

FIGURE 8 Flame height correlation.

gas-phase phenomena. Consequently, the data will be analyzed over the peak burning conditions of the sample and the corresponding flame heights and heat fluxes will be reported. The transient behavior of the solid will be characterized by a burning time which will also be reported.

Peak burning conditions were somewhat arbitrarily defined as follows:

1) the maximum value recorded by the first heat flux sensor (at x_1) was located, and the times at which 80 percent of this maximum first occurred on either side of the peak were located;

2) average values for each heat flux sensor were determined for these times, *i.e.*,

$$\bar{q}_i'' = \frac{1}{(t_2 - t_1)} \int_{t_1}^{t_2} q_i'' \, dt; \tag{13}$$

3) this procedure was also applied to the corresponding flame height measurements;

4) a similar procedure was applied to the energy release rate data of Walton and Twilley (1984) for the same materials, but evaluated at somewhat higher external radiative heating conditions.

The burning time (t_b) was defined by locating the times bounding the peak heat flux for the sensor at x_1 at which the flux was 10 percent of its maximum. These

"80 percent peak-average" values and the burn times are tabulated in Table I for the heat transfer experiments. The energy release rates were interpolated from the peak values plotted in Figure 7 as derived from Walton and Twilley (1984).

Flame height Figure 8 displays the height of the visible flame tips with the energy release rate per wall fire width, $\dot{E}' = \dot{E}'' x_p$. Although the data trend follows the correlations of Hasemi (1984) and Delichatsios (1984), there is considerable scatter. For the most part, the scatter is believed due to the inconsistency in deriving flame height and energy release from two independent devices. It does not necessarily mean that these devices are incompatible, except where a horizontal burn configuration was used in the calorimeter for the flexible foam material. The scatter does suggest that greater care in data accuracy and interpretation is needed when x_f is nearly equal to x_p in magnitude, when the burning time is short, and when the composite nature of the sample produces multiple effects during combustion. All of these factors probably contributed to the carpet, aircraft panel and rigid foam samples. Also, a visible observation of transient flaming is probably not ideal for a flame height measurement although consistency among several observers was noted.

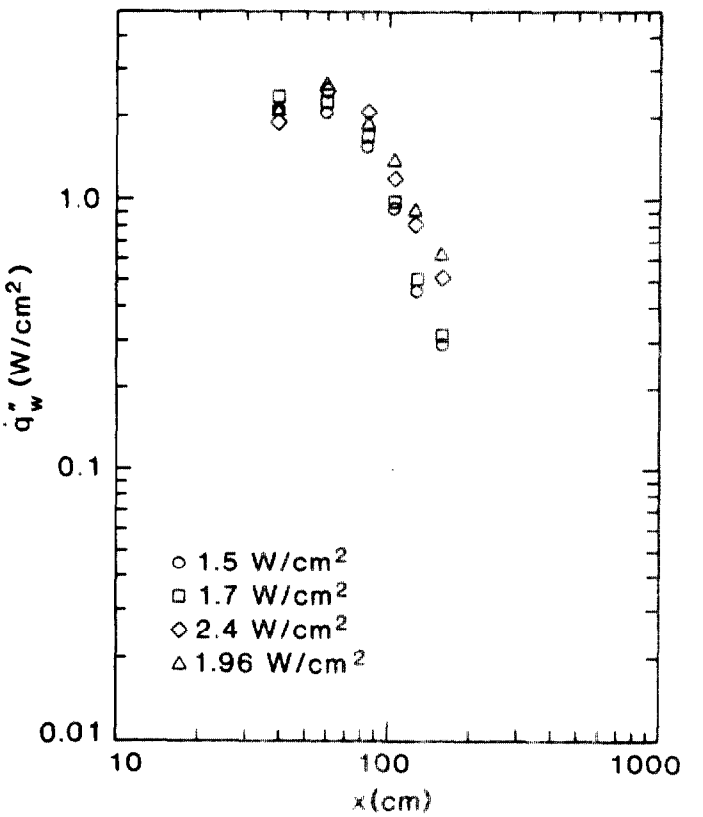

FIGURE 9a Wall heat flux distribution—PMMA.

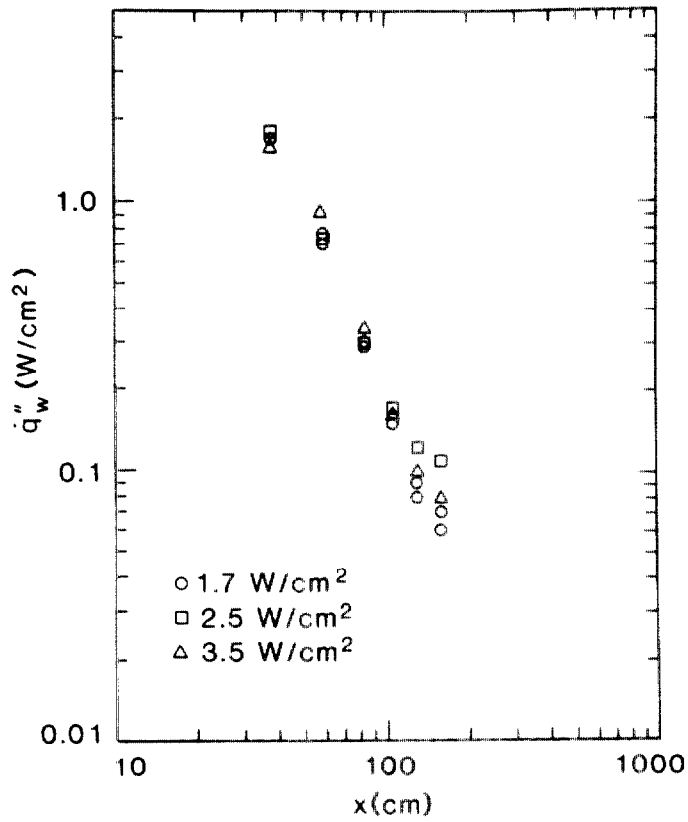

FIGURE 9b Wall heat flux distribution—particleboard.

It is interesting, and essential for the development of numerical results, to determine ε, the ratio of oxygen present to stoichiometric oxygen needed for complete combustion. This is a mixing factor that represents the inability for the entrained oxygen to react instantly with the fuel available. From Eq. (5) and the coefficient given by Hasemi for the flame tips in Eq. (6), ε is computed as 6.6 for $Y_{ox,\infty}=0.233$, *i.e.*, air. Tamanini (1977) computes a corresponding value of 9 for a turbulent axisymmetric flame plume, but such values (*e.g.*, 5 to 20) are abundant in the literature. Nevertheless, the parameter ε is a valuable fluid dynamic modeling parameter. If the coefficient for the continuous flame height is used instead, *i.e.*, 2.9 in Eq. (6), then ε becomes 3.13. Thus, the theory suggests that about 3 times the stoichiometric air is entrained over the continuous combustion region, and 6.6 times stoichiometric air is entrained over the entire combusting zone to the flame tip.

Wall heat flux The wall total heat flux distributions are presented in Figures 9a through 9f for each of the materials. The distance x is measured from the base of the

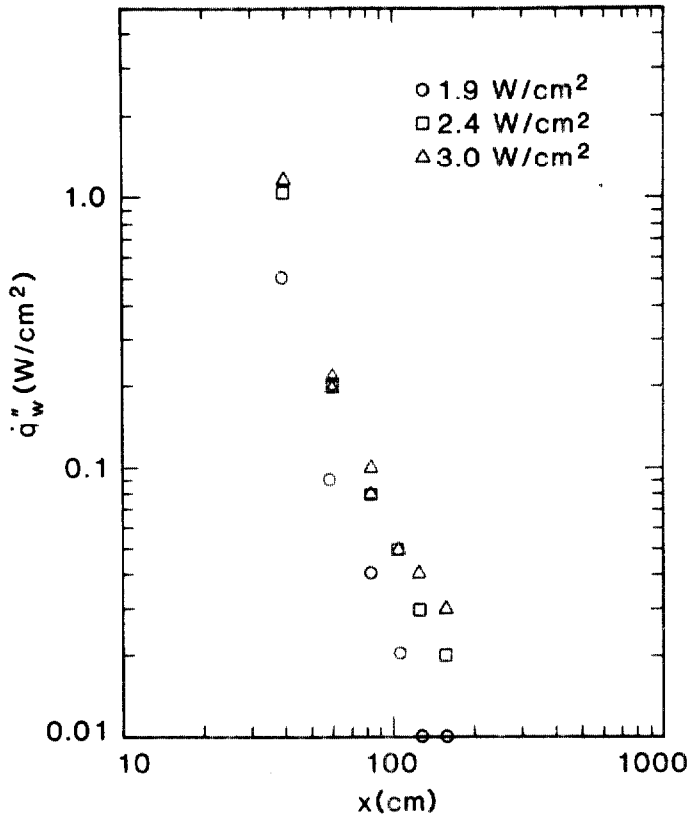

FIGURE 9c Wall heat flux distribution—rigid foam.

sample as indicated in Figure 1. The effect of the external irradiance level is not marked, probably because the change in energy release rate inferred from Figure 7 is not large enough. Also transient and particular material characteristics must have some bearing here. For the most part the materials display a decreasing flux with distance, $\dot{q}_w'' \propto x^{-p}$ where p is about 2.4. This is consistent with the distributions measured by Ahmad and Faeth (1979) outside of the flame zone, and can be approximately described by the model offered by Liburdy and Faeth (1978). In the case of PMMA, the flux displays a maximum or nearly constant value of 2 to 3 W/cm² in the flame zone. This is indicative of the combustion zone results found by Ahmad and Faeth (1979). Indeed, the level of heat flux in this combusting region is similar despite the different fuels.

As a result of this observation it was thought appropriate to scale the distance x with the flame length x_f in considering the flux distribution. Such an analysis was performed by Hasemi (1984) for CH_4 line burner fires against a wall with $\dot{E}'$ ranging from about 10 to 100 kW/m. Also he reprocessed the data of Ahmad and Faeth

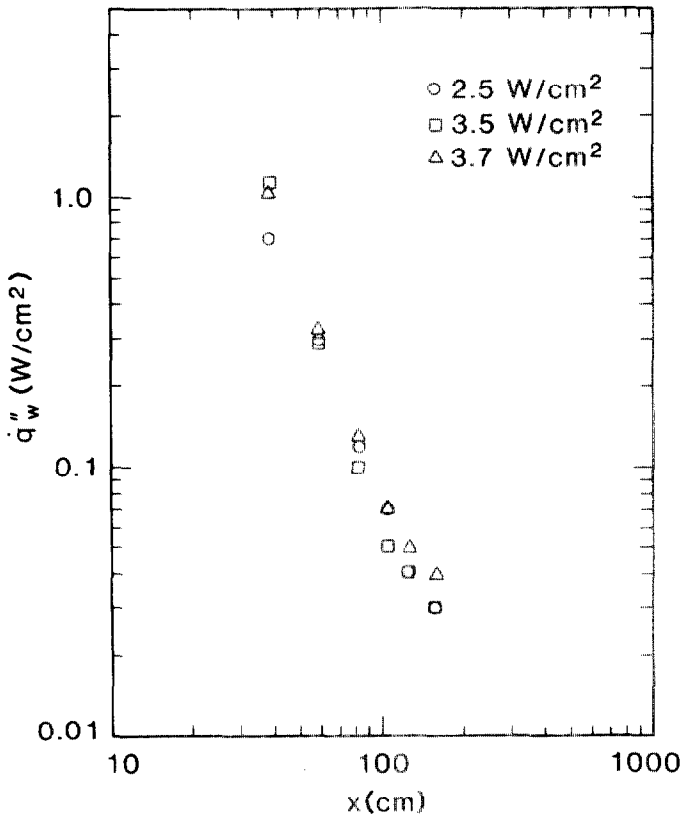

FIGURE 9d Wall heat flux distribution—flexible foam.

(1979) into this form; and those results, along with a sample of Hasemi's data in the apparatus of Figures 1 and 2, are shown in Figure 10. No definitive understanding of the effects of fuel type, fuel configuration and energy release have been extracted from these results at this time. The universality of the correlation with the displayed scatter is intriguing and bears further study.

As a consequence of the burner analysis the data of Figure 9 were plotted in terms of x/x_f with the result shown in Figure 11. This approach does significantly collapse the data and the results are consistent with the correlation in Figure 10. The maximum values of recorded heat flux for each material range from about 1 to slightly less than 3 W/cm². Thus a universal maximum value does not seem apparent as the data correlation might imply. Either more data need to be derived within the flame region for the materials yielding low maximum fluxes, or the flux distribution depends on energy release rate. The latter factor is suggested by the theoretical analysis as expressed by Eq. (9) in that $\dot{q}_w'' \propto (\dot{E}'')^{1/3}$. This was explored further by plotting $\dot{q}_w''/(\dot{E}'')^{1/3}$ from Table I against x/x_f for the materials. The result is shown in Figure

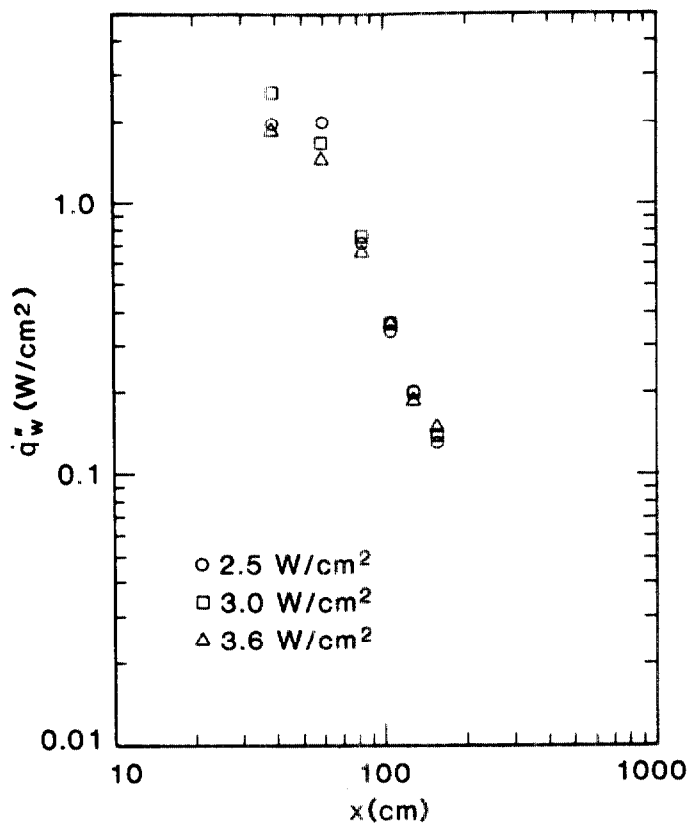

FIGURE 9e Wall heat flux distribution—carpet.

12, and seems to offer no improvement over Figure 11 although the maximum value of $\dot{q}_w''/(\dot{E}'')^{1/3}$ is nearly identical for four of the materials. Moreover, the scatter here is likely due to the same inconsistencies in the flame height correlation of Figure 8 in which the extrapolated energy release data may be at fault.

Finally, the theoretical solution for heat flux will be examined. If χ_r, the radiative fraction, is selected as 0.20 suggestive of natural gas and $Y_{ox,\infty}=0.233$ (air), it can be shown that β of Eq. (9b) is computed as

$$\beta = (9.81 + 17.7)(\dot{E}')^{1/3}/\varepsilon \ (\mathrm{kW/m^2}), \tag{14}$$

where 9.81 represents the convective contribution and 17.7 represents the radiative contribution (with $\dot{E}'$ in kW/m) (Figure 13). Preliminary assessments of the radiative component of the wall heat flux has suggested its contribution to be approximately 50 percent for natural gas. These theoretical results give 64 percent for $\chi_r=0.20$. Thus the radiative effects appear to be crudely computed, although the x-dependence of the heat flux is not correctly represented in the flame zone.

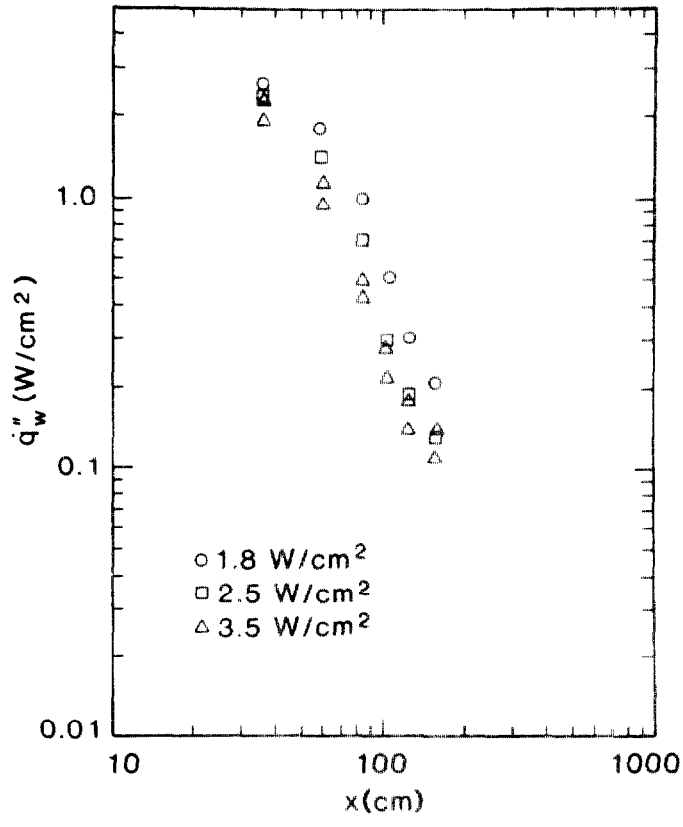

FIGURE 9f Wall heat flux distribution—aircraft panel.

Flame Spread Characteristics

A first step has been taken to characterize heat transfer from wall flames so that upward flame spread might be predicted. It is obvious that additional study needs to be given to complete this objective, but the current results offer at least a framework for analysis. Ultimately a prediction of the transient burning rate or energy release rate is also needed, and models have not been developed for this aspect. Nor has it been shown how results from laboratory calorimetry data can be utilized in such analyses. Some additional data can be presented for the materials considered herein which address some aspects of related flame spread phenomena. For example, downward or lateral spread in air on a vertical surface can be expressed from Quintiere and Harkleroad (1984) as follows:

$$V = \frac{\Phi}{(k\rho c)(T_{ig} - T_s)^2}, \quad T_{s,\min} \leq T_s < T_{ig}, \tag{15}$$

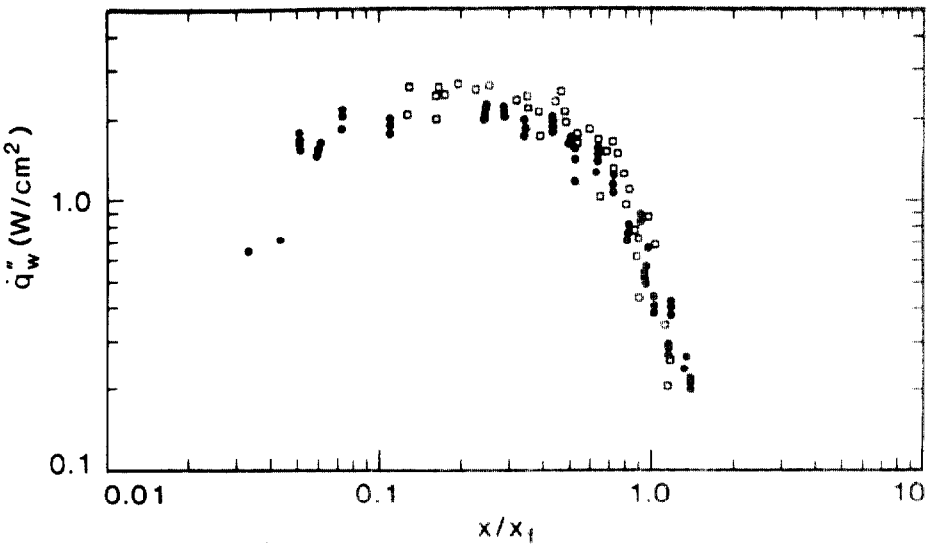

FIGURE 10 Wall heat flux for steady wall fires correlated with flame height. ●, CH_4 line burner flames (Hasemi, 1984). □, Liquid saturated wall fires (Ahmed and Faeth, 1979).

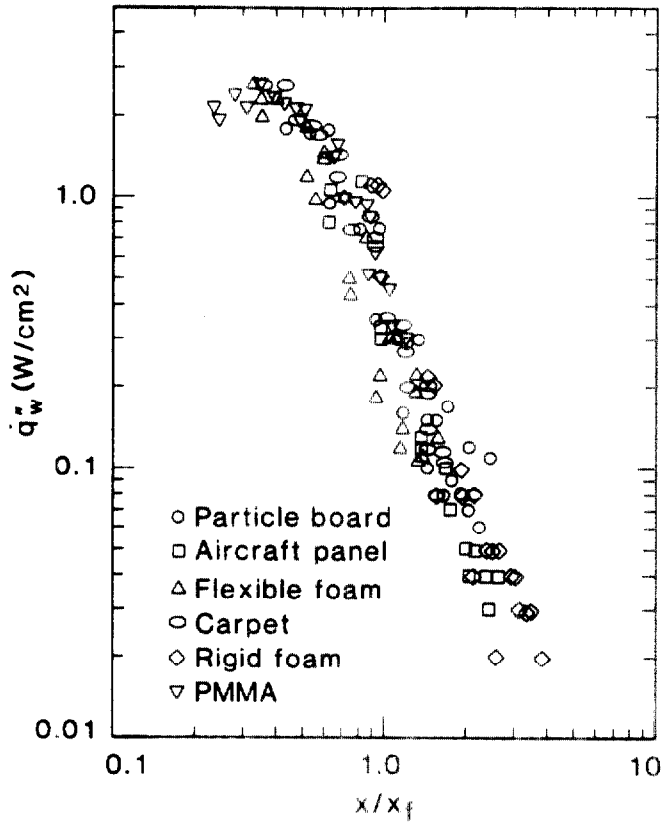

FIGURE 11 Wall heat flux correlated using flame height.

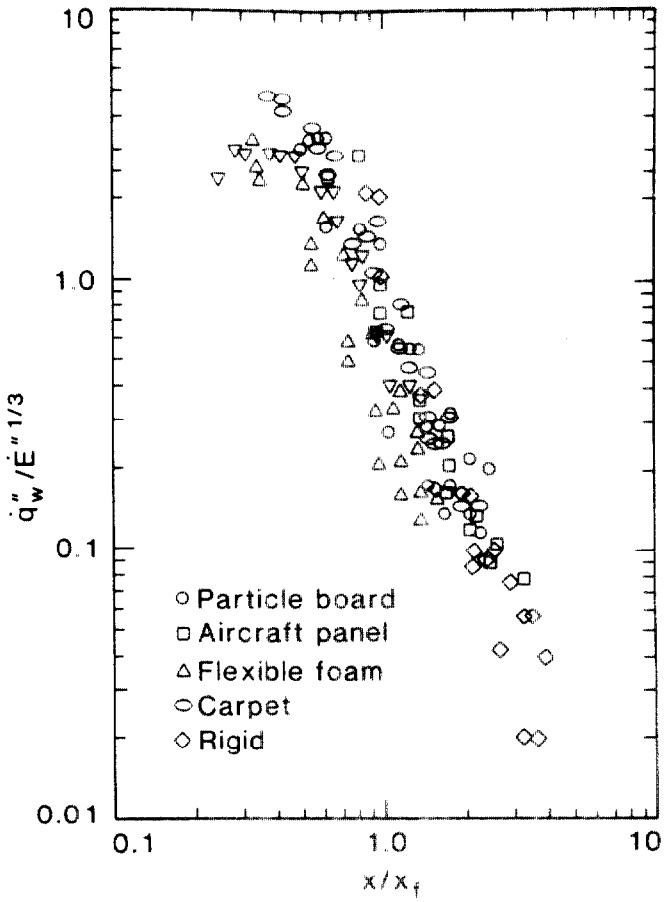

FIGURE 12 Wall heat flux correlated using flame height and energy release rate.

where Φ represents a flame heat transfer parameter,
$k\rho c$ is the effective thermal inertia of the solid,
T_{ig} is the effective ignition (piloted) temperature,
T_s is the upstream surface temperature, and
$T_{s,\min}$ is the minimum surface temperature necessary for flame spread.

Pyrolysis rate might be approximated as

$$\dot{m}'' = \frac{\dot{q}_{s,\text{net}}''}{L}, \tag{16}$$

where $\dot{q}_{s,\text{net}}''$ is the net surface heat flux which is related to $\dot{q}_w''$, but not exactly identical, due to blowing effects and surface re-radiation; L is the effective heat of gasification. Finally, the energy release rate is given as

$$\dot{E}'' = \dot{m}'' \Delta H, \tag{17}$$

with ΔH the heat of reaction.

TABLE II

Material flame spread properties

Material	Ref.:	T_{ig} +1 °C	$k\rho c$ 1 $(kW/m^2\,K)^2\,s$	Φ 1 $(kW)^2/m^3$	$T_{s,min}$ 1 °C	ΔH 2 (kJ/g)	L 2 (kJ/g)	r 2 (gO_2/g fuel)	ΔH 3 (kJ/g)	L 3 (kJ/g)	$T_{s,b}$ 3 °C
Particleboard		412	0.93	4.27	275	11.6	4.5	0.89	12.4[b]	1.7[b]	457[b]
Aircraft panel		505	0.24	0	505	17.6	3.7	1.34	—	—	—
Flexible foam		390	0.32	11.7	120	18.8	—	1.44	16[a]	1.96[a]	457[a]
Carpet		412	0.68	11.1	265	16.8	2.5	1.28	—	—	—
Rigid foam (GM31)		435	0.03	4.09	215	21.0	7.8	1.6	13	3.1	517
PMMA		378	1.02	14.4	≤ 90	25.6	1.8	1.95	22–25	1.6	387

[a]Different flexible foam, GM-21.
[b]Different wood, oak.
+1. Quintiere and Harkleroad (1984).
2. Walton and Twilley (1984).
3. Tewarson (1980).

Values for these parameters are summarized in Table II. Also some attempt at comparison is made there with similar data by Tewarson (1980). An effective comparison is made there with similar data by Tewarson (1980). An effective stoichiometric oxygen to fuel ratio and Tewarson's surface temperature at steady burning $T_{s,b}$ are also given. The values for the rigid foam material (GM-21) show the most disparity between the work of Walton and Twilley (1984) and Quintiere and Harkleroad (1984) with those by Tewarson (1980). Also, ignition results, not shown, reflect similar disagreement. This is a fire retardant foam that has been stored in a material bank (Nadeau, 1980) for several years. Tewarson used the material in the mid-1970s and our use has been in the last several years. Thus some material change might have occurred, since so many of the compared parameters are different. Of course this is speculation, but could prove an issue for interlaboratory comparisons on material performance.

Although no direct measurements of upward flame spread were made, Eq. (12) suggests some flame spread characteristics. A spread time t_f can be computed based on the maximum wall heat flux recorded for each run. This can be compared to the burn time t_b and its ratio t_f/t_b suggests a propensity to spread. If this ratio is small

TABLE III

Propensity for flame spread

Material	$\dot{q}_e''$ (W/cm²)	$t_f = (k\rho c)[(T_{ig} - T_\infty)/\dot{q}''_{w,max}]^2$ (s)	t_f/t_b (−)
Particleboard	1.7	484	1.1
Douglas Fir (1.27 cm)	1.7	478	2.3
	2.5	400	1.9
	3.4	441	1.1
Flexible foam (2.54 cm)	1.8	63	0.9
	2.5	78	1.4
	3.5	109	2.4
	3.5	82	1.7
Carpet	2.5	264	2.0
(nylon/wool blend)	3.0	150	1.5
	3.0	290	2.9
	3.6	147	1.4
Rigid foam, GM-31	1.9	197	7.03
(2.54 cm)	2.4	46	0.4
	3.0	41	0.3
	3.0	39	0.3
PMMA, Type G	1.5	277	0.2
	1.7	224	0.1
	2.4	205	0.2
	3.0	185	0.2
Aircraft panel	2.5	874	20
(epoxy fiberite)	3.0	446	15
	3.7	498	18

then continued spread is likely, and conversely. These results are shown in Table III. A more complete understanding of the transient effects together with a more complete solution to Eqs. (10) and (11) is necessary. Temporarily at least some appreciation of the phenomenon can be discerned from t_f/t_b.

CONCLUSIONS

Heat transfer from wall flames has been addressed both theoretically and experimentally. Although too simplified to accurately describe the processes, the theoretical model does give the observed flame height characteristics, and does suggest the form and variables important to flame heat transfer.

A direct measure of energy release rate is a necessary addition to the heat transfer apparatus. This can probably be best done with the current design by the addition of a load cell to measure mass loss together with a separate measure of ΔH.

Also a direct measure of the radiative component of the wall heat flux must be achieved. Several approaches need to be tried here to arrive at a consistent and direct technique. Finally an improved engineering analysis must be developed to address the radiative component.

Two key results emerge from this study. First, flame height for wall flames is primarily proportional to the energy release rate to the 2/3-power, albeit scatter exists in our material data. Second, wall heat flux seems to have an approximately universal distribution when plotted with distance normalized by flame length (x/x_f); however, energy release rate and radiation effects could mitigate this universality. These results hold at least for the turbulent flames of this study; namely, 0.3 to 1.4 m in height. For larger wall flames, flame radiation will dominate the heat flux and this correlation should begin to break down.

ACKNOWLEDGEMENTS

The authors wish to acknowledge Mr. W. Rinkinen and Mr. D. Wagger for their support in conducting the heat transfer experiments, and Mr. K. Steckler who contributed to the design of the experimental apparatus. Special recognition is given to Prof. A. Kulkarni of the Pennsylvania State University who served as a summer faculty participant in the initial experimental phase of this work. Also we wish to thank Dr. T. Eklund as the technical monitor for the Federal Aviation Administration Technical Center and their support which contributed to this study.

REFERENCES

Ahmad, T., and Faeth, G. M. (1979). *Seventeenth Symposium (International) on Combustion*, The Combustion Institute, pp. 1149–1160.

Alpert, R. L. (1983). Pressure modeling of fire growth on char-forming and laminated materials. FMRC J.I. 0G0-N3.BU, RC83-BT-11, Factory Mutual Res. Corp.

Chedaille, J., and Brand, Y. (1972). *Measurements in Flames*, Vol. 1 of *Industrial Flames*, J. M. Beer and M. W. Thring (Eds.). Int. Flame Res. Foundation, Crane, Russak and Co., Inc., New York.

deRis, J. N. (1969). *Twelfth Symposium (International) on Combustion*. The Combustion Institute, pp. 241–252.

Delichatsios, M. A. (1984). Modeling of aircraft and cabin fires. NBS-GCR-84-473, Nat. Bur. Stand.

Delichatsios, M. A. (1984a). Flame heights in turbulent wall fires with significant flame radiation. *Comb. Sci. and Tech*, **39**, 195.

Gardon, R. (1953). *The Review of Scientific Instruments*, Vol. 24, No. 5.

Harkleroad, M., Quintiere, J., and Walton, W. (1983). Radiative ignition and opposed flow flame spread measurements on materials. U.S. Dept. Trans., Fed. Aviation Admin. Tech. Ctr., DOT/FAA/CT-83/28.

Hasemi, Y. (1984). *Fire Science and Technology*, Vol. 4, No. 2, p. 75.

Hognon, B. (1983). Behavior in fire of interior wall coverings and linings. Centre Scientifique et Technique du Bâtiment, France.

Lee, B. T. (1984). Standard room fire test development at the National Bureau of Standards. Symp. on Application of Fire Science to Fire Engineering, Amer. Soc. Testing and Materials/ Soc. Fire Prot. Engrs., Denver.

Liburdy, J. A., and Faeth, G. M. (1978). *J. Heat Trans.*, **100**, No. 2, Amer. Soc. Mech. Engrs.

Nadeau, H. G. (Ed.) (1980). *Materials Bank Compendium of Fire Property Data*, Products Research Comm.

Orloff, L., deRis, J., and Markstein, G. H. (1975). *Fifteenth Symposium (International) on Combustion*, The Combustion Institute, p. 183.

Parker, W. J. (1982). An assessment of correlations between laboratory and full-scale experiments for the FAA Aircraft Fire Safety Program, Part 3: ASTM E 84, NBSIR 82-2564, Nat. Bur. Stand.

Quintiere, J. (1982). An assessment of correlations between laboratory and full-scale experiments for the FAA Aircraft Fire Safety Program, Part 4: Flammability tests, NBSIR 82-2525, Nat. Bur. Stand.

Quintiere, J., Harkleroad, M., and Walton, D. (1983). Measurement of material flame spread properties, *Comb. Sci. Tech.* **32**, 67.

Quintiere, J. G., and Harkleroad, M. (1984). New concepts for measuring flame spread properties. Symp. on Application of Fire Science to Fire Engineering, Amer. Soc. Testing and Materials/Soc. Fire Prot. Engrs., Denver.

Quintiere, J. (1985). Some factors influencing the fire spread over room linings and in the ASTM E 84 Tunnel Test. *Fire and Materials* **9**, No. 2, p. 65.

Saito, K., Williams, F. A., and Quintiere, J. (1985). Upward turbulent flame spread. *First International Symposium on Fire Safety Science*, Hemisphere Publishing Co. (to be published).

Sarkos, C. P., Hill, R. G., and Howell, W. D. (1982). The development and application of a full-scale wide-body test article to study the behavior of interior materials during a post-crash fuel fire. AGARD, Aircraft Fire Safety Lecture Series No. 123, France, NATO.

Sibulkin, M., and Kim, J. (1977). *Comb. Sci. and Tech.* **17**, 39.

Smith, E. E., and Satija, S. (1981). Release rate model for developing fires. Amer. Soc. of Mech. Engrs., ASME Paper No. 81-HT-4.

Sparrow, E. M., and Cess, R. D. (1978). *Radiation Heat Transfer*, Hemisphere Pub. Co./McGraw-Hill Book Co.

Steckler, K. D. (1983). Calculations of wall fire spread in an enclosure. Nat. Bur. Stand., NBSIR 83-2765.

Tamanini, F. (1977). *Combustion and Flame* **30**, 85.

Tamanini, F. (1979). *Seventeenth Symposium (International) on Combustion*, The Combustion Institute, p. 1075.

Tewarson, A. (1980). Physico-chemical and combustion pyrolysis properties of polymetic materials. NBS-GCR-80-295, Nat. Bur. Stand.

Walton, W. D., and Twilley, W. H. (1984). Heat release and mass loss rate measurements for selected materials. NBSIR 84-2960, Nat. Bur. Stand.

NOMENCLATURE

a	parameter, Eq. (18)
b	parameter, Eq. (19)
c, c_p	specific heat
C_e	entrainment coefficient
C_f	friction coefficient
E	energy release by chemical reaction
g	gravitational acceleration
k	thermal conductivity (used in flame spread analysis)

L effective heat of gasification, Eq. (40)
m mass of fuel gasified
Pr Prandtl number
q heat transferred
r effective stoichiometric oxygen/fuel mass ratio
St Stanton number
t time
T temperature
u, v gas phase velocity components
V spread velocity
x, y coordinates
Y mass fraction
z normalized y coordinate, Eq. (9)

Greek Symbols

β heat transfer parameter, Eq. (36)
δ characteristic length
ΔH heat of reaction per mass of fuel
ΔH_{ox} heat of reaction per mass of oxygen
ε mixing factor
η dimensionless variable, (z/δ)
χ thermal conductivity (in heat transfer analysis)
ρ density
τ shear stress
χ_r radiative fraction of E
θ $T-T_\infty$
Φ flame heating parameter, Eq. (39)

Subscripts

b burnout
c convective
e external
f flame
g gas
ig ignition
m maximum
ox oxygen
p pyrolysis
r radiative
s surface
w wall
∞ ambient

Superscripts

$(\dot{})$ per unit time
$()'$ per unit length
$()''$ per unit area
$()'''$ per unit volume

Appendix A

CONVECTIVE HEATING EFFECTS ON A THIN FOIL HEAT FLUX SENSOR

The sensor was a circular foil heat flux gage of the type described by Gardon (1953). It consists of a thin constantan foil of radius R and thickness S, and was purchased commercially. The exposed surface is blackened and had an emissivity of approximately 0.98 in this case. The body and therefore the edge of the foil was maintained at a cool temperature (T_w) by water flow.

To estimate the effect of convective heat transfer the following assumptions and analysis were made.

1) No heat losses from the back face of the foil.

2) No re-radiation from the front face of the foil.

3) Uniform irradiance $\dot{q}_e''$, gas temperature T_∞, and convective heat transfer coefficient h are assumed.

The governing equation for the foil heat transfer is

$$\frac{d}{dr}\left(r\frac{d\phi}{dr}\right) - m^2 r\phi = 0, \tag{A-1}$$

$$r = R, \quad \phi = T_w - T_\infty - \dot{q}_e''/h,$$

$$r = 0, \quad \frac{d\phi}{dr} = 0,$$

where $\phi = T - T_\infty - \dot{q}_e''/h$

$m = \sqrt{(h/kS)}$

k = thermal conductivity of the foil.

The response of a thermocouple measuring the foil center to edge temperature difference is related to the heat flux by

$$T(0) - T_w = [\dot{q}_e'' + h(T_\infty - T_w)]\left(\frac{1 - 1/I_0(mR)}{h}\right), \tag{A-2}$$

where I_0 is a Bessel function. For small mR, $I_0 \sim 1 + (1/2mR)^2$ or

$$T(0) - T_w \cong [\dot{q}_e'' + h(T_\infty - T_w)]\frac{m^2 R^2}{4h} = [\dot{q}_e'' + h(T_\infty - T_w)]\frac{R^2}{4kS}. \tag{A-3}$$

Equation (A-3) is equivalent to the pure radiation results in which $h \equiv 0$, and also under conditions of mR small, convection is directly additive. Moreover, the calibration constant of the sensor is not dependent on its calibration technique or its

application with respect to convective or radiative heating provided mR is small, or h does not vary significantly for the conditions of calibration and application.

The values of mR for the sensors used, with $h=7$ W/m² K determined in calibration with a radiant source and hot water (47°C), can be computed as follows:

$$R = 0.217 \text{ cm} = 2.17 \times 10^{-3} \text{ m},$$
$$S = 0.0025 \text{ cm} = 2.5 \times 10^{-5} \text{ m},$$
$$k = 21.6 \text{ W/m}^2 \text{ K},$$

and $mR=0.25$. This is small enough for Eq. (A-3) to hold with good accuracy. Moreover, under the natural convection conditions of this experiment, it is not expected that h will vary markedly.

Appendix B

RADIATIVE ANALYSIS FOR A HOMOGENEOUS WALL FLAME

For a non-uniform temperature wall flame represented as a constant thickness slab, infinite in extent with the wall and ambient temperatures equal to T_0, it can be shown (Sparrow and Cess, 1978) that the radiative flux is given as

$$\dot{q}_r''(y) = 2\left\{B_1 E_3(\tau) - B_2 E_3(\tau_0 - \tau) + \int_0^{\tau} \sigma T^4 E_2(\tau - t)dt - \int_0^{\tau_0} \sigma T^4 E_2(t - \tau)dt\right\}, \quad \text{(B-1)}$$

where E_2 and E_3 are exponential integral functions. The position y is measudre from the wall, B_1 and B_2 are the bounding surface radiosities both equal to δT_0^4, and

$$\tau = \int_0^y \kappa dy, \quad \text{(B-2)}$$

$$\tau_0 = \int_0^{\delta} \kappa dy, \quad \text{(B-3)}$$

with κ the absorption coefficient of the flame and δ is its thickness.

The wall flux ($y=0$) for $\tau_0 \ll 1$, *i.e.*, optically thin, can be written as

$$\dot{q}_{r,w}'' = 2\int_0^{\tau_0} \sigma T^4 dt + 2\tau_0 \sigma T_0^4, \quad \text{(B-4)}$$

since $E_3 \sim 1/2 - \tau$ and $E_2 \sim 1$. In this case the last term is small and may also be dropped. An identical expression results for the flux at the free boundary interface, which implies that the flame radiation splits equally in both directions.

Appendix C

A SIMPLE ANALYTIC SOLUTION TO AN IDEALIZED LINE-FUEL-SOURCE WALL FIRE

As a first approximation a simple model is put forth to provide a framework for approaching an analysis of the data and for identifying points for further study. The model will only deal with the effects in the reacting zone, and the chemical effects will be treated only as a source of energy in the energy equation. Thus diffusion of species will not be explicitly included nor will pyrolysis effects of the solid. The fuel might be considered to originate at a line-source so that we attempt to simulate flame heating of the downstream non-pyrolyzing region. In fact, the surface temperature of the solid will be treated as uniform and at the ambient temperature T_∞, since the surface temperature will be much less than the flame temperatures. A schematic of the posed problem is shown in Figure 5. The two-dimensional governing equations follow:

$$\frac{\partial(\rho u)}{\partial x} + \frac{\partial(\rho v)}{\partial y} = 0, \tag{C-1}$$

$$\rho\left(u\frac{\partial u}{\partial x} + v\frac{\partial u}{\partial y}\right) = g(\rho_\infty - \rho) + \frac{\partial}{\partial y}\left(\mu\frac{\partial u}{\partial y}\right), \tag{C-2}$$

$$\rho c_p\left(u\frac{\partial \theta}{\partial x} + v\frac{\partial \theta}{\partial y}\right) = \frac{\partial}{\partial y}\left(\lambda\frac{\partial \theta}{\partial y}\right) + \frac{\partial \dot{q}_r''}{\partial y} + \dot{q}''', \tag{C-3}$$

where $\theta = T - T_\infty$, $\dot{q}_r''$ is the radiative flux, and $\dot{q}'''$ is the energy release due to chemical reaction, with the boundary conditions:

$$\begin{aligned} y = 0, \quad & \theta = u = v = 0, \\ y \to \infty, \quad & \theta = u = 0. \end{aligned} \tag{C-4}$$

These equations are integrated over $0 \le y < \infty$ to yield, from Eq. (C-2):

$$\frac{d}{dx}\int_0^\infty \rho u^2\, dy = \int_0^\infty g(\rho_\infty - \rho)dy - \tau_w, \tag{C-5}$$

where $\tau_w = \mu(du/dy)_{y=0}$, the wall shear stress.

Similarly, integration of Eq. (C-3) gives

$$c_p\frac{d}{dx}\int_0^\infty (\rho u\theta)dy = -\dot{q}_{w,c}'' - \dot{q}_r'' + \int_0^\infty \dot{q}'''\, dy, \tag{C-6}$$

where $\dot{q}_{w,c}'' = \lambda(d\theta/dy)_{y=0}$, the convective heat flux to the wall, and $\dot{q}_r''$ is the flame radiative heat loss. It is further assumed that the flame is optically thin, which implies that $\dot{q}_r''$ can be assumed equally split between the wall and the environment. The mass and enthalpy additions of the fuel have been neglected since we expect these source terms to be small compared with the total mass and energy transfers over the flame region, *i.e.*, $\dot{m}'$ is small compared to $(\rho v)_{y=\infty}$, the air entrained. Furthermore, the

energy release rate will be based on the oxygen consumption rate, *i.e.*,

$$\int_0^\infty \dot{q}''' dy = -\frac{(\rho v)_{y\to\infty} \cdot Y_{ox,\infty}}{\varepsilon r} \Delta H = -(\rho v)_{y\to\infty} \frac{Y_{ox,\infty} \Delta H_{ox}}{\varepsilon}, \tag{C-7}$$

where ΔH_{ox} is the heat of reaction per unit mass of oxygen consumed (approximately 13 kJ/g for most hydrocarbons), and ε is a mixing factor implying that some oxygen is not immediately reacted.

In addition, the flame radiation will be assumed as a constant fraction χ_r of the energy release,

$$\dot{q}_r'' = \chi_r \int_0^a \dot{q}''' dy. \tag{C-8}$$

Tamanini (1979) demonstrated that this is not as good as using a "soot-band" model, but his results suggest that it is not an unreasonable approximation. The wall component is then

$$\dot{q}_{w,r}'' = \dot{q}_r''/2 \tag{C-9}$$

for the optically thin case. A more suitable expression based on the radiation transfer equation is given in Appendix B, but will not be pursued here.

In order to eliminate the density dependence the following transformation is made,

$$z = \int (\rho/\rho_\infty) dy. \tag{C-10}$$

The integral equations then become

$$\rho_\infty \frac{d}{dx} \int_0^\infty u dz + (\rho v)_{y\to\infty} = 0, \tag{C-11}$$

$$\rho_\infty \frac{d}{dx} \int_0^\infty u^2 dz = \int_0^\infty \rho_\infty g \frac{\theta}{T_\infty} dz - \tau_w, \tag{C-12}$$

$$\rho_\infty c_p \frac{d}{dx} \int_0^\infty u\theta dz = \rho_\infty Y_{ox,\infty} \frac{\Delta H_{ox}}{\varepsilon} (1-\chi_r) \frac{d}{dx} \int_0^\infty u dz - \dot{q}_{w,c}'' \tag{C-13}$$

where $\mu/\rho = \mu_\infty/\rho_\infty$, $k/\rho c_p = k_\infty/\rho_\infty c_p$, and c_p are all assumed constant.

The equations can be integrated and solved by introducing the profiles,

$$u = u_1(x) F(\eta), \tag{C-14a}$$

$$\theta = \theta_1(x) G(\eta), \tag{C-14b}$$

where $\eta = z/\delta(x)$ and δ is the boundary layer thickness. Also u and θ are taken to be zero for $\eta > 1$.

Following Liburdy and Faeth (1978) for the high Reynolds number regime of a turbulent wall plume,

$$(\rho v)_{y\to\infty} = -\rho_\infty C_e u_m, \tag{C-15}$$

$$\tau_w = C_f(\rho_\infty u_m^2/2), \tag{C-16}$$

$$\dot{q}''_{w,c} = St(\rho_\infty c_p u_m \theta_m), \tag{C-17}$$

with the local maximum, $u_m = au_1$ and $\theta_m = b\theta_1$; and where C_e (the entrainment constant), C_f (the friction coefficient), and St (the Stanton number) are all constant. Also, by the Coburn analogy,

$$St = Pr^{-2/3} C_f/2. \tag{C-18}$$

$$\begin{aligned} u_1 &= u_0 x^{1/2}, \\ \theta_1 &= \theta_0, \\ \delta &= \delta_0 x \end{aligned} \tag{C-19}$$

and

can satisfy Eqs. (C-11) to (C-13). Upon substitution Eq. (C-11) yields:

$$\delta_0 = \frac{2}{3} aC_e / \int_0^1 F\, d\eta; \tag{C-20}$$

Eq. (C-12) yields:

$$u_0^2 \delta_0^2 \int_0^1 F^2\, d\eta = \frac{g\delta_0 \theta_0}{T_\infty} \int_0^1 G\, d\eta - \frac{C_f a^2 u_0^2}{2}; \tag{C-21}$$

and Eq. (C-13) yields:

$$c_p \theta_0 \delta_0 \frac{3}{2} \int_0^1 FG\, dy = \frac{Y_{ox,\infty} \Delta H_{ox} (1 - \chi_r)\delta_0}{\varepsilon} \frac{3}{2} \int_0^1 F\, d\eta - \frac{c_p abC_f Pr^{-2/3} \theta_0}{2}. \tag{C-22}$$

Reasonable profiles, to satisfy the boundary conditions and the physical behavior suggested by analogous problems, were taken as

$$F(\eta) = \eta^{1/7}(1 - \eta) \tag{C-23}$$

and

$$G(\eta) = \eta(1 - \eta)^2, \tag{C-24}$$

for which at $\eta = 0$, $u = \theta = 0$ and at $\eta = 1$, $u = \theta = \partial\theta/\partial\eta = 0$ as well as the 1/7-power holds for u near the wall. It follows that $a = 7/8^{8/7} = 0.650$ and $b = 4/27 = 0.148$. Consequently, the solutions for δ_0, u_0, and θ_0 are

$$\delta_0 = 1.06 C_e, \tag{C-25}$$

$$\theta_0 = \frac{1.99 a \theta_f C_e}{0.408 aC_e + abC_f / Pr^{2/3}}, \tag{C-26}$$

where

$$\theta_f \equiv Y_{ox,\infty} \frac{\Delta H_{ox}}{\varepsilon} (1 - \chi_r)/c_p;$$

and

$$u_0 = 0.52aC_e\left\{\frac{g\theta_f}{T_\infty(0.675aC_e + a^2C_f/2)(0.408aC_e + adC_f/Pr^{2/3})}\right\}^{1/2}.$$

Liburdy and Faeth (1978) give results that suggest $C_e = 0.096$ for $C_f = 0.015$ and $Pr = 0.7$. Thus a solution is found.